www.lajss.org
Latin American Journal of Solids and Structures 5 (2008) 1–15

2D bending field of variable thickness floating ice floes loaded upon impact to an inclined wall

João B. de Aguiar*

Sistemas Mecânicos, Escola Politécnica, USP – Brazil

Abstract

In some circumstances ice floes may be modeled as beams. In general this modeling supposes constant thickness, which contradicts field observations. Action of currents, wind and the sequence of contacts, causes thickness to vary. Here this effect is taken into consideration on the modeling of the behavior of ice hitting inclined walls of offshore platforms. For this purpose, the boundary value problem is first equated. The set of equations so obtained is then transformed into a system of equations, that is then solved numerically. For this sake an implicit solution is developed, using a shooting method, with the accompanying Jacobian. In-plane coupling and the dependency of the boundary terms on deformation, make the problem non-linear and the development particular. Deformation and internal resultants are then computed for harmonic forms of beam profile. Forms of giving some additional generality to the problem are discussed.

Keywords: variable thickness beam, contact forces, elastic foundation, internal resultants

1 Introduction

Ice floes that may be characterized as beams occur in nature in diverse forms. Width is never constant and thickness, specially, presents variations, [1]. It is therefore not realistic to model contact problems with offshore platforms, assuming constancy of thickness. This simplification, however, allows a close form of solution to the problem [3].

The particular way an ice floe geometry changes has been considered under diverse points of view, included the dynamic one [8]. Invariably, starting from a perfect ice formation, driven by wind, currents and waves, constructed models show how impact, lateral and frontal, builds thickness variations in the ice floe. These variations result in general not symmetrical, leading to a curved equal area plane. Furthermore observed motion and contact conduct to 2D compressive-flexural problems. However the effect of these geometrical quantities is never analyzed in detail and 1D beam situations are usually considered [11].

Moreover, usual analysis misses the fact that the behavior of ice, upon contact with inclined walls of offshore platforms [10], induces deformation dependency of the loading terms. Justification given is that objective is the construction of simple first order models. Alternatively,

*Corresp. author email: jbaguiar@usp.br Received 13 Mar 2007; In revised form 15 Aug 2007

use of available numerical codes, like the finite element method, under the semi-infinite characterization of the problem is also approximate, as thickness variations are not embodied in their library elements [4].

Given the situation, a model is developed here to take into account some of these different restrictions. In it, first the boundary value problem is presented and then a system transformation of the obtained equations performed. It follows a two-point numerical scheme, addressing the solution of the resulting equations, completed with a 3D generalization of the procedure, that come as an additional tool of analysis.

2 Formulation

2.1 Boundary value problem

Upon contact with the inclined wall of an offshore platform, every element of the ice foe, supposed having constant width b_0 but variable height h,$h(y) = \bar{h}t$, while floating as a result of buoyancy, Fig. 1, will be under the action of internal resultants $< N, M, V >$ that obey [2]:

$$\begin{array}{l} \partial_{,y}(N) \cong 0 \\ \partial_{,y}(V) - b\gamma_{sw} w \cong 0 \\ \partial_{,y}(M) - V + N\partial_{,y}(w + w_i) \cong 0; \qquad \partial_{,y} = \frac{d}{dy} \end{array} \tag{1}$$

Axial equilibrium, as conveyed by normal force N, is described by the first equation, whereas lateral equilibrium between shear component V and buoyancy forces, dependent of foundation coefficient γ_{sw}, is considered in the second. Third equation relates to rotational equilibrium. Additionally quasi-static conditions of loading are admitted and inertia effects discarded, given the time frame of many observed events. The longitudinal form of the equal area axis, e.a.a., w_i is supposed derived from the thickness profile.

Early in the winter, ice floes present an elastic brittle behavior, therefore if this fact is brought to the modeling an isotropic elastic constitutive relationship may be assumed. Hence $M = -E'I\,\partial_{,yy}(w)$ and $N = E'A\partial_{,y}(v)$; $A = b_0 h$. Here the pair $< v, w >$ comprises the axial and lateral displacements, respectively. Under these circumstances, the set of differential equations of equilibrium, d.e.e., above combines into a single statement:

$$\partial_{,yy}[(\frac{t}{t_0})^3 \partial_{,yy}(w)] + 4\gamma_0^4 \partial_{,yy}(w) + 4\delta_0^4 w = -4\gamma_0^4 \partial_{,yy}(w_i) \tag{2}$$

which depends on the coefficients,

$$\gamma_0 = (\frac{n_0}{4E'i_0})^{\frac{1}{4}}; \qquad n_0 \geq 0 \text{ and } \delta_0 = (\frac{\gamma_{sw}}{4E'i_0})^{\frac{1}{4}} \tag{3}$$

being n_0 the value of the normal force per unit width at the origin, $n_0 = \frac{N_0}{b_0}$, which then makes up the coupling term γ_0. The thickness h may be written about its mean value

$\bar{h}$; $\bar{h} = < h > = \lim_{L\to\infty} \frac{\int_0^L h(y)dy}{L}$, by means of the thickness profile function t, so that $h = \bar{h}t$. Finally $i_0 = \frac{I_0}{b_0}; I = bh^3/12$ is a second moment per unit width term at the origin. Equivalent beam Young's modulus E' is introduced to take into account one-dimensional behavior of wide floes and as such for the narrow case, setting $\nu = 0$ converts plate equation above into a beam one. Hence,

$$i_0 = \frac{h_0^3}{12} = \frac{\bar{h}^3 t_0^3}{12} \qquad E' = \frac{E}{(1-\nu^2)} \tag{4}$$

Here E is the elastic modulus of the material and ν its Poisson's ratio. Value of the $t = t(y)$ at origin is t_0.

For the case where the beam is loaded at the origin by a shear force and a bending moment, both associated to the in-plane resultant n_0, as it occurs when an inertia driven ice floe encounters a fixed offshore platform wall, loading introduced by the contact at this end may be described by

$$\begin{array}{ll} y = 0; & m_0 = -E' i_0 \partial_{,yy}(w)_0 \\ & v_0 = -E' i_0 \partial_{,yyy}(w)_0 - \frac{3}{t_0}\partial_{,y}(t)_0 m_0 - n_0 \partial_{,y}(w + w_i)_0 \end{array} . \tag{5}$$

These equations relay on the free parameter n_0, related to the solution of the in-plane problem. They also reveal dependence upon the deformation of the beam at the origin. Boundary statement at the other end, the far end, requires that regularity conditions be satisfied:

$$\begin{array}{ll} y \to \infty; & w_\infty = 0 \\ & \partial_{,y}(w)_\infty = 0 \end{array} . \tag{6}$$

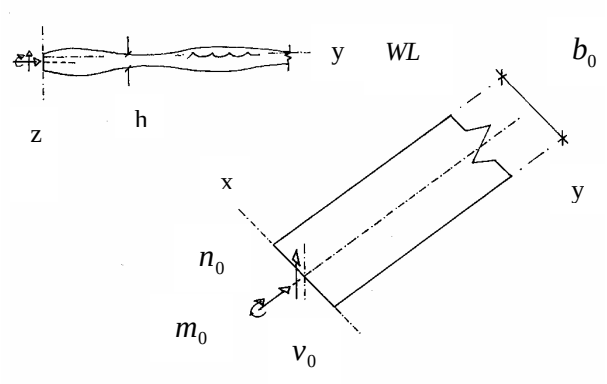

Figure 1: Beam element with thickness variation.

2.2 System of equations

Solution of the fourth order d.e.e. shown above, Eq. (2), subjected to the stated boundary conditions, b.c., Eqs. (5)-(6), may be accomplished by a transformation of this equation into

a set of four equations. Relationship among derivatives is established by a matrix if vector $\mathbf{u}$, containing displacements, rotations, curvatures and rate of curvature, is defined:

$$\mathbf{u}^T = \lfloor \; w \quad \partial_{,y}(w) \quad \partial_{,yy}(w) \quad \partial_{,yyy}(w) \; \rfloor; \quad w = \hat{w}_t(y; b.t.) \tag{7}$$

Here row form representation is used and dependency with position and boundary terms, b.t., admitted. In particular, interface rotation $\theta_0 = \partial_{,y}(w)_0$, resulting from local deformation, will determine the left end loading.

With the above definition, equilibrium statement will take the form of a system of equations:

$$\{u'\} = [K]\{u\} + \{u_i\}; \qquad u'_n = \partial_{,y}(u_n); \qquad n = 1, 2, 3, 4 \tag{8}$$

where the matrix $[K]$ and vector $\{u_i\}$ comprises the elements,

$$[K] = \begin{bmatrix} 0 & 1 & 0 & 0 \\ 0 & 0 & 1 & 0 \\ 0 & 0 & 1 & 0 \\ -\frac{4\delta_0^3}{t^3}t_0^3 & 0 & -\frac{6t[\partial_{,y}(t)]^2+3t^2\partial_{,yy}(t)+4\gamma_0^4 t_0^3}{t^3} & -\frac{6\partial_{,y}(t)}{t} \end{bmatrix} ; \{u_i\} = \begin{bmatrix} 0 \\ 0 \\ 0 \\ \frac{-4\delta_0^4 t_0^3}{t^3}\partial_{,yy}(w_i) \end{bmatrix} \tag{9}$$

Boundary terms should conform as well. Considered the proper equivalent form, boundary statements follow from Eqs. (5)-(6) and can be cast into the form:

$$\{\varphi\} = [A]\{u_0\} + [B]\{u_L\} - \{\alpha\} - \{\beta\}; \qquad \{\varphi\} = \{0\} \tag{10}$$

where the matrices $[A]$ and $[B]$ are such that:

$$[A] = \begin{bmatrix} 0 & 0 & 0 & 0 \\ 0 & 0 & 0 & 0 \\ 0 & 0 & E'i_0 & 0 \\ 0 & n_0 & 0 & E'i_0 \end{bmatrix}; \qquad [B] = \begin{bmatrix} 1 & 0 & 0 & 0 \\ 0 & 1 & 0 & 0 \\ 0 & 0 & 0 & 0 \\ 0 & 0 & 0 & 0 \end{bmatrix} \tag{11}$$

whereas the vectors $\{\alpha\}$and $\{\beta\}$, in row form, will be:

$$\lfloor\alpha\rfloor = \lfloor \; 0 \quad 0 \quad m_0 \quad v_0 - m_0\frac{3\partial_{,y}(t)_0}{t_0} \; \rfloor; \quad \lfloor\beta\rfloor = \lfloor \; 0 \quad 0 \quad 0 \quad -n_0\partial_{,y}(w_i)_0 \; \rfloor \tag{12}$$

which then completes the system of equations to be solved.

2.3 Numerical solution

Solution of the above system depends, for every value of n_0, on the determination of the exact $\{u\}$ vector that makes $\{\varphi\}$ null for specified values of the left and right end vectors. It should be kept in mind, however, that in general these values may depend upon the behavior of the beam, and as such are not exactly known a priori. A numerical trial and error type of approach may

then be applied, using a Newton scheme of solution. Specifically: trial vectors are chosen to set conditions at the left end of the interval $[0, L)$. It comprises an iteration sequence intended the matching of the correct boundary conditions at the other end of the beam, the right end.

Hence, in the iterative process, if at iteration j, of an open set on which a convergence criterion sets the stop point M,

$$\{\varphi^j\} \neq \{0\}; \qquad \{\varphi^j\} = [A]\{u_0^j\} + [B]\{u_N^j\} + \{\alpha^j\} - \{\beta^j\}; \qquad j = 1, 2, ..., M \tag{13}$$

over a discretized space containing $N+1$ stations $\{y_i\};\ i = 0, 1, 2, ..., N$, being

$$\{u_0^j\} = \{u^j(y_0)\}; \qquad \{u_N^j\} = \{u^j(y_N)\}; \quad y_0 = 0; \quad y_N = L; \quad \forall j \tag{14}$$

then requiring that the boundary conditions in the next iteration be met is equivalent to asking for an increment that makes:

$$\{\varphi^{j+1}\} = \{0\}; \qquad \{\varphi^{j+1}\} = [A]\{u_0^{j+1}\} + [B]\{u_N^{j+1}\} + \{\alpha^{j+1}\} - \{\beta^{j+1}\} \tag{15}$$

being $\Delta\{u_0^{j+1}\}$ the required vector increment. If this is so, then

$$\Delta\{u_o^{j+1}\} = -[\partial_{\{u_0^{j+1}\}}(\varphi_N^{j+1})]^{-1} \cdot \{\varphi_N^j\} \tag{16}$$

where, from Eq. (15), the partial derivative with respect to the trial vector is

$$[\partial_{\{u_0^{j+1}\}}\{\varphi^{j+1}\}] = [A][I] + [B][\partial_{\{u_0^{j+1}\}}\{u_N^{j+1}\}] + [\partial_{\{u_0^{j+1}\}}\{\alpha^{j+1}\}] - [\partial_{\{u_o^{j+1}\}}\{\beta^{j+1}\}] \tag{17}$$

which depends, in its middle term, on the derivative at the far end (station N, numerically), through a transfer matrix. Here $[I]$ is the identity matrix. Application of the chain rule as:

$$[\partial_{\{u_0^{j+1}\}}\{u_N^{j+1}\}] = [\partial_{\{u_{N-1}^{j+1}\}}\{u_N^{j+1}\}]\,[\partial_{\{u_{N-2}^{j+1}\}}\{u_{N-1}^{j+1}\}]...[\partial_{\{u_1^{j+1}\}}\{u_2^{j+1}\}]\,[\partial_{\{u_0^{j+1}\}}\{u_1^{j+1}\}] \tag{18}$$

requires a Taylor expansion to relate the derivatives

$$\{u'^j_{n+1}\} = \{u'^j_n\} + \partial_{,y}\{u'^j_{n+1}\}\Delta y \tag{19}$$

This is a truncated-to-first-term series whose calculation requires the computation of a tangent modulus. A Backward Euler Method [5] may be chosen to compute this term. Though a little bit more complicated it has the advantage of being unconditionally stable. Taking this route and noticing from Eq.(8) that

$$\{u'^j_{n+1}\} = [K_{n+1}]\{u_{n+1}^j\} + \{u_i\}_{n+1}\,; \qquad [K_{n+1}] = [K(y_{n+1})] \tag{20}$$

allows that the result be combined with Eq. (19) to produce:

$$\{u_{n+1}^{j+1}\} = [T_n^{n+1}]\{u_n^{j+1}\} + [M_{n+1}]^{-1}\{\Delta N_{n+1}\} - [M_{n+1}]^{-1}\{\Delta u_i\}\,; \tag{21}$$

where

$$[T_n^{n+1}] = [M_{n+1}]^{-1}\,[K_n] \tag{22}$$

that does not depend upon the iteration number. It relates vectors at successive stations. In it the section matrix

$$[M_{n+1}] = ([I] - \Delta y\,[K'_{n+1}]\,[K_{n+1}^{-1}] - \Delta y\,[K_{n+1}])\,[K_{n+1}]; \qquad [K'_{n+1}] = \partial_{,y}[K_{n+1}] \tag{23}$$

appears in its inverse form. This form depends on parameters of the medium, sectional properties, loading as well as material variables. Also in Eq. (21):

$$[\Delta N_{n+1}] = [K_{n+1}]\,\{u_i\} + \{u'_i\} \tag{24}$$

$$\{\Delta u_i\} = \{u_i\}_{n+1} - \{u_i\}_n \tag{25}$$

Finally an operational form may be constructed from the above results and Eq. (21). It is the complete transfer matrix, for the iteration at hand, in product form:

$$[T_0^N] = \prod_{n=0}^{N-1} [T_n^{n+1}]; \tag{26}$$

It takes the individual transfer matrices between consecutive stations, with partitions

$$[T_n^{n+1}] = [\{t_l\}_m]; \quad l, m = 1, 2, 3, 4 \tag{27}$$

whose coefficients are polynomial expressions of the discretization step;

$$\{t\}_1 = \left\{ \begin{array}{c} Ab\Delta^2 y + Ac\Delta y - A \\ ab\Delta^3 y + ac\Delta^2 y - a\Delta y \\ ac\Delta y^3 + [Bb - b^2 - bc' + b'c - a]\Delta^2 y + [Bc - bc - b']\Delta y + [b - B] \\ -a\Delta y^3 + [Cb - bc - b']\Delta y^2 + [Cc - c' - c^2]\Delta y + [c - C] \end{array} \right\} \tag{28}$$

for the first column,

$$\{t\}_2 = \left\{ \begin{array}{c} -Aa\Delta y^3 \\ [ab' - a'b]\Delta y^3 + [ac' - a'c + ab]\Delta y^2 + [a' + ac]\Delta y - a \\ [ac' - a'c + ab - aB]\Delta y^3 + [a' + aC]\Delta y^2 - a\Delta y \\ [a' + ac - Ca]\Delta y^3 - a\Delta y^2 \end{array} \right\} \tag{29}$$

for the second,

$$\{t\}_3 = \left\{ \begin{array}{c} -Aa\Delta^2 y \\ -a^2\Delta y^3 \\ [ac' + ab - a'c - Ba]\Delta y + [a' + ac]\Delta y - a \\ [a' + ac - Ca]\Delta y^2 - a\Delta y \end{array} \right\} \tag{30}$$

for the third, and

$$\{t\}_4 = \left\{ \begin{array}{c} -Aa\Delta y \\ -a^2\Delta^2 y \\ -a^2\Delta y^3 + [a'b - ab']\Delta^2 y - aB\Delta y \\ [a' + ac - aC]\Delta y - a \end{array} \right\} \tag{31}$$

for the last. In these matrices terms $< a, b, c >_l$ were defined according to: $a_l = -\frac{4\delta_0^4}{t_l} t_0^3$, for $a_n = A \wedge a_{n+1} = a$, whereas $b_l = -\frac{6t_l[\partial_{,yy}(t)]_l^2 + 3t_l^2[\partial_{,yy}(t)]_l + 4\gamma_0^4 t_0^3}{t_l^3}$ with $b_n = B \wedge b_{n+1} = b$ and finally $c_l = -6\frac{[\partial_{,y}(t)]_l}{t_l}$ for $c_n = C \wedge c_{n+1} = c$, being $l = 1, 2, ..N$ and $' \equiv \partial_{,y}$. Once the transfer matrix is computed, for the iteration in case, the Jacobian, Eq. (17), can be calculated:

$$[J^{j+1}] = [A]\,[I] + [B]\,[T_0^N] + \frac{\partial\{\alpha^{j+1}\}}{\partial\{u_0^{j+1}\}} - \frac{\partial\{\beta^{j+1}\}}{\partial\{u_0^{j+1}\}} \tag{32}$$

which allows the calculation of an increment $\Delta\{u_0^j\}$, Eq. (16). Convergence measure for finite length L rests on the hypothesis that $w_L \leq K_w$ and $\partial_{,y}(w)_L \leq K_\theta$, where $< K_w, K_\theta >$ are suitably small constants.

3 Application

3.1 Loading

The impulse generated by the inertia change of the ice floe when it contacts the inclined wall of the offshore platform produces flexure, shear and compression at the interface. The rate of change of the linear momentum **l** equals the sum of the external forces, normal and shear, per unit width at the interface:

$$\mathbf{l}(\tau) = \int_{\mathbf{0}}^{\infty} \mathbf{v}(\tau)\rho_i h dy; \qquad \dot{l}_y = n_{\mathbf{0}}; \quad \dot{l}_z = -v_0 \tag{33}$$

while the rate of change of the angular momentum **a** equals the resultant interface moment:

$$a_x(\tau) = \int_0^{\infty} \dot{\theta}(\tau)\,\rho_i i_0 dy; \quad \dot{a}_x = m_0 \tag{34}$$

These expressions depend on linear $v^T = \lfloor\ \dot{v} \quad \dot{w}\ \rfloor$, and angular $\dot{\theta}$**,** velocities, being $\rho_i = \frac{\gamma_i}{g}$ the specific mass of the ice. However, due to the fact that in the scenario of events, loading is very slow, its time frame surpasses by far duration time of dynamic effects, granting then use of quasi-static analysis.

Values of normal n_0, bending moment m_0 and shear force v_0 at the interface depend on the contact between platform and beam [6]. They are resultants described by the coefficient of friction μ between ice and the rigid wall of the platform, its slope angle ϕ and the coefficient of eccentricity ζ, Fig. 2. Solving the normal $r_0\mathbf{e}_n$ and tangential $\mu r_0\mathbf{e_t}$ to the inclined wall in terms of its horizontal and vertical components

$$z_0 = r_0(\cos\phi - \mu\sin\phi); \qquad y_0 = r_0(\sin\phi + \mu\cos\phi) \tag{35}$$

and denoting the rotation at the origin by θ_0, it results that:

$$\begin{aligned} n_0 &= -z_0\sin\theta_0 + y_0\cos\theta_0 \\ v_0 &= z_0\cos\theta_0 + y_0\sin\theta_0 \\ m_0 &= -n_0 e \end{aligned} \tag{36}$$

being $e = \zeta h_0; --0.50 \leq \zeta \leq 0.50$ the eccentricity. The coefficient μ depends on the existence of sliding or sticking contact conditions, for every value of r_0. An additional consideration has to be introduced here, as the shear force at the origin v_0 will also depend on the direction of the motion of the beam. For the riding-up condition, or up-slope case, under slipping and sticking regimes, putting $\rho = \tan^{-1}\mu$ into Eq. (36) gives:

$$\begin{aligned} v_0 &\leq n_0\tan(\phi_t); \qquad \phi_t \leq \rho \\ v_0 &\leq n_0\tan(\phi_t - \rho); \qquad \phi_t \geq \rho \end{aligned} \tag{37}$$

where ρ is a material parameter, related to the way the ice and wall interact, and dependent on surface roughness and temperature among other factor. Term ϕ_t is $\theta_0 + \phi$. Notice that deformation of the beam acts to create an effective value of friction angle. Table 1 presents the values considered in the present analysis. Aspect ratios $h_0/b_0 = \{1, 2, 4\}$ were considered in the simulations presented ahead.

Table 1: Set of parameters used in the analysis.

Loading and Geometric Parameters	
Slope angle set, degrees	$\phi = \{15, 30, 45\}$
Eccentricity set	$\zeta = \{$-0.5, 0, 0.5$\}$
Friction coefficient set	$\mu = \{0.05, 0.25\}$

3.2 Material parameters

Ice is a quite complex material, whose constitutive equation depends on the type of microstructure considered, time of the year, form of response sought, etc. For ice features in a brittle state, in salt water, Table 2 presents some average values of the properties of this material [12] and [9]. Foundation coefficient was set to the density of salt water, $\gamma_{sw} = 1.0045e + 4\text{Pa/m}$.

Table 2: Some properties of the beam material.

Properties of Ice	
Elastic modulus, Pa	$E = 0.50e + 10$
Poisson's ratio	$v = 0.30$
Flexural strength, MPa	$S_f = 0.70$
Compressive strength, MPa	$S_c = 5.0$

3.3 Contact variables

In the field, the monitored variable r_0, the intensity of contact, has to be used in assessing the interface normal n_0. However, because the displacements do depend on the interface conditions, loading at origin depends on the rotation $\theta_0 = \partial_{,y}(w)_0$, Eqs. (12) and (34):

$$\frac{\partial\left\{\alpha^{j+1}\right\}}{\partial\left\{u_0^{j+1}\right\}} = \begin{bmatrix} 0 & 0 & 0 & 0 \\ 0 & 0 & 0 & 0 \\ 0 & 0 & \frac{\partial m_0^{j+1}}{\partial\theta_0^{j+1}} & 0 \\ 0 & \frac{\partial v_0^{j+1}}{\partial\theta_0^{j+1}} - 3\frac{\partial m_0^{j+1}}{\partial\theta_0^{j+1}}\frac{\partial_{,y}(t)_0}{t_0} & 0 & 0 \end{bmatrix} \tag{38}$$

where,

$$\frac{\partial m_0^{j+1}}{\partial\theta_0^{j+1}} = -r_0 e\{\cos(\phi)[\mu\cos(\theta_0^{j+1}) - \sin(\theta_0^{j+1})] - \sin(\phi)[\cos(\theta_0^{j+1}) - \mu\sin(\theta_0^{j+1})]\} \tag{39}$$

and,

$$\frac{\partial v_0^{j+1}}{\partial\theta_0^{j+1}} = r_0\{\cos(\phi)[\cos(\theta_0^{j+1}) + \mu\sin(\theta_0^{j+1})] + \sin(\phi)[-\sin(\theta_0^{j+1}) + \mu\cos(\theta_0^{j+1})]\} \tag{40}$$

Moreover,

$$\frac{\partial\beta^{j+1}}{\partial u_0^{j+1}} = \begin{bmatrix} 0 & 0 & 0 & 0 \\ 0 & 0 & 0 & 0 \\ 0 & 0 & 0 & 0 \\ 0 & -\frac{\partial n_0^{j+1}}{\partial\theta_0^{j+1}}\partial_{,y}(w_i)_0 & 0 & 0 \end{bmatrix} \tag{41}$$

where:

$$\frac{\partial n_0^{j+1}}{\partial\theta_0^{j+1}} = -\frac{1}{e}\frac{\partial m_0^{j+1}}{\partial\theta_0^{j+1}} \tag{42}$$

Therefore guessing the entrance values for the u_0^{j+1} vector requires that the curvature $\kappa_0^{j+1} = \partial_{,yy}(w^{j+1})_0$ be such that $\kappa_0^{j+1} = -\frac{m_0^{j+1}}{E'i_0}$, where m_0^{j+1} does depend on the guessed value of θ_0^{j+1},

according to the above, and it does not represent a free choice. The same can be said of the rate of curvature at the origin, $\partial_{,y}(\kappa^{j+1})_0$ that should obey the equation for shear force at the interface, Eq.(5).

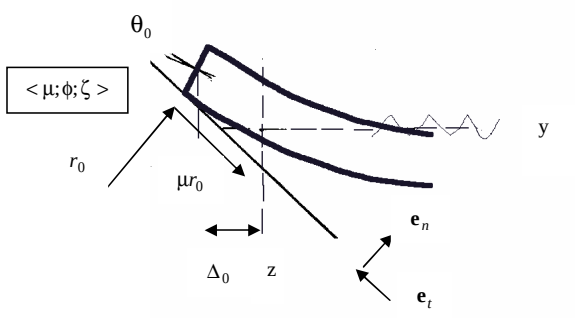

Figure 2: Interface point contact situation.

4 Results

The numerical procedure presented above was coded into a Fortran routine and cases corresponding to some particular beams run. The procedure, though based in an implicit scheme, resulted in a code with fast rate of convergence. Results presented ahead, for the bending moment diagrams, come from the implementation of this routine. The profile of the beam, as set forth by the $t = t(y)$ function, is considered of harmonic form, as it is generated by the action of waves and wind, mostly. A general term of this description may be written as $t = 1 + \frac{a_t}{h}\sin(\kappa_t y + \psi_t)$ being a_t the amplitude, $k_t = \frac{2\pi}{\lambda_t}$ the wave number, λ_t the wave length and ψ_t the phase angle. Upper and lower side thickness variations may be conceived, resulting in symmetric and anti-symmetric thickness variations, and therefore straight and harmonic equal area axes, Figs. 3 and 4. Here only pure thickness variation effects, as uncoupled from irregularities of the equal area axis, are studied. Table 3 shows the values adopted for these geometric variables.

Effect of the amplitude of the variations of the beam thickness on the bending moment distribution, fixed all parameters but the amplitudes, may be represented by a function $m = \hat{m}_{t/a_t}(y; n_0; a_t, \lambda_t, \psi_t)$ in Figure 5 for ${}^{h_0}/_{b_0} = 2$ and ${}^{\lambda_t}/_{\lambda_0} = 0.125; \psi_t = 0$, with boundary terms set by $\langle \phi = 30, \mu = 0.05, \zeta = 0.50 \rangle$. In this plot moments are normalized with respect to the failure bending moment $m_f = \frac{2iS_f}{h}$, being S_f the flexural strength of ice, whereas positions along the beam are normalized with the wave-like factor $\lambda_0 = \frac{2\pi}{\delta_0}$. In-plane loads are normalized with the crushing load, $n_c = S_c h$. It shows a strong dependence of the bending moments on the amplitude of the thickness variation function. In particular it should be pointed out the closeness of the point of occurrence of the maximum bending moment with the position of minimum thickness.

Table 3: Set of profile parameters used in the analysis.

Geometric Profile	
Relative Amplitudes	$\frac{a_t}{h} = \{0;\ 0.0625;\ 0.125;\ 0.1875\}$
Relative Length	$\frac{\lambda_t}{\lambda_0=\{\infty,0.500,0.125\}}$
Phase Angle	$\Psi_t = \{0.; 30; 60; 90\}$

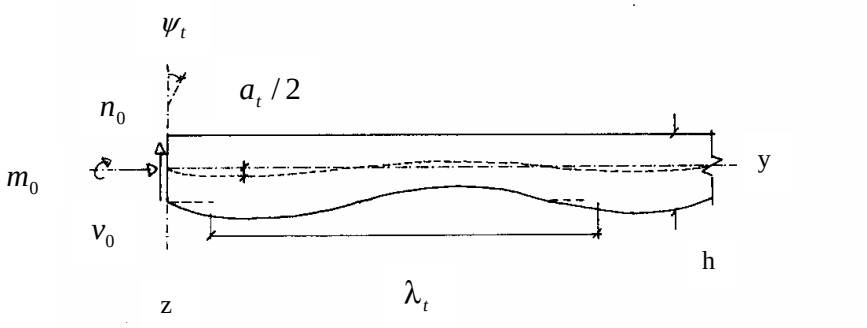

Figure 3: Anti-symmetrical thickness variation profile: e.a.a. curved.

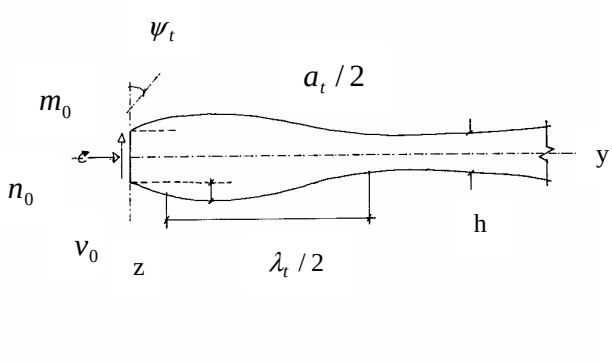

Figure 4: Symmetric thickness variation profile: e.a.a. straight.

Dependence of the bending moment field upon the wave length of the thickness profile is measured by $m = \hat{m}_{t/\lambda_t}(y; n_0; a_t, \lambda_t, \psi_t)$ and the results are presented in Figure 6 for ${}^{a_t}/_{h_0} = 0.0625$, $\psi_t = 0$ and the same boundary terms of above. Negligible effects on bending moments occur at lengths of the order of λ_0. Truly null effects, however, only occur when $\lambda_t \to \infty$. But, extreme values of bending moments occur, again, at points close to minimum sectional thickness. Additionally, because shorter wave lengths will bring the sections of minimum thickness closer to the loading region, they will also be more effective in bringing up the extreme values of the bending moments.

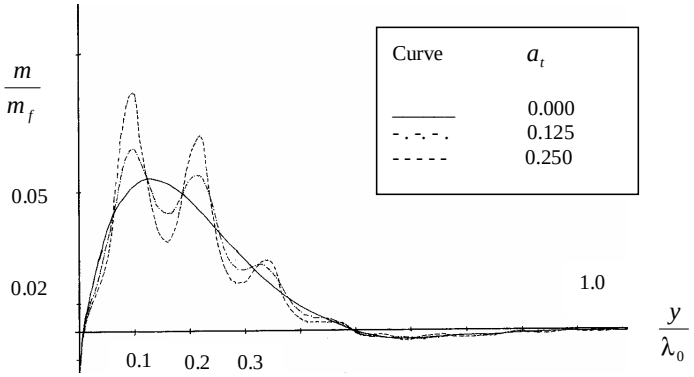

Figure 5: Effect of amplitude of thickness variation on bending moments.

Finally, a shift of phase angle ψ_t increases the extreme values m_e of bending moments when it brings the sections of minimum thickness closer to the loading region, as it is drawn in Figure 7 for $m = \hat{m}_{t/\psi_t}(y; n_0; a_t, \lambda_t, \psi_t)$. In it boundary terms are conserved and ${}^{a_t}/_{h_0} = 0.0625; {}^{\lambda_t}/_{\lambda_0} = 0.125$. An opposite effect will be observed when it affects the first neck of the beam in an opposite sense.

Overall, extreme values of bending moment $m_e = \hat{m}(y_e; n_0; a_t, \lambda_t, \psi_t)$, fixed the loading, and geometry, occur at values y_e^m such that $\partial_{,y}(m)_{y_e^m} = 0$. Finding this position requires an internal loop added to the above procedure, as the value y_e^m will not, in general, coincide with any discretized position y_n. Therefore, after an initial search that delimits this position, $y_m \leq y_e^m \leq y_{m+1}$, an approximate Newton procedure will find $\Delta y = y_e^m - y_m$ from $\Delta y = -\frac{\partial_{,y}(m)_{y_m}}{\partial_{,yy}(m)_{y_m}}$.

5 Discussion and conclusion

Formulation presented above permits different expansions. Thickness variation profiles present a stocastic character. Nonetheless development of the different profiles based on the sum of harmonic functions allows a very close representation of the observed forms. Therefore, from Eq. (2), it is clear that if $t = \sum_l t_l; \quad t_l = \hat{t}_l(y; a_l, \lambda_l, \psi_l)$ then solution will involve sum of responses, not linear, but that can be obtained from the presented procedure. Care must be

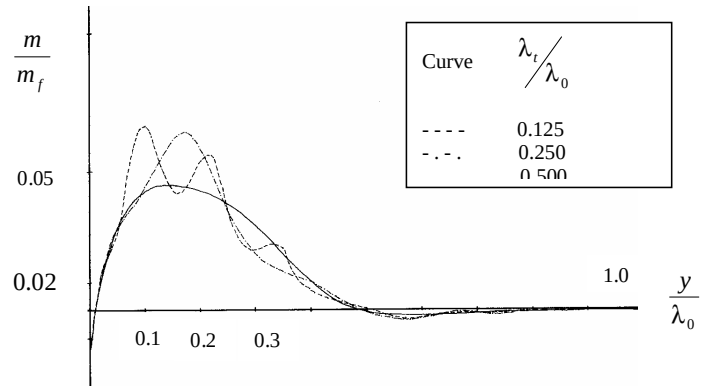

Figure 6: Effect of wave-length of thickness variation on bending moments.

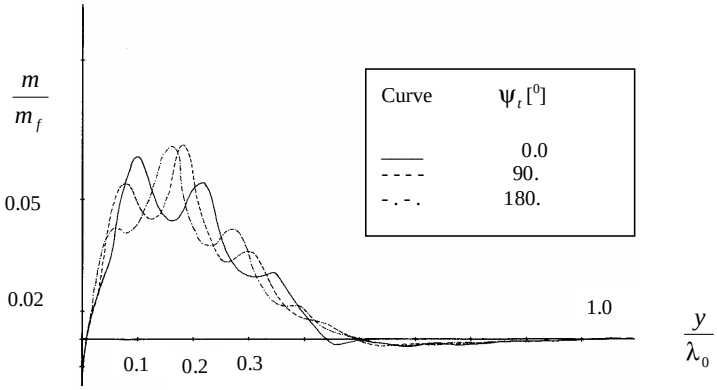

Figure 7: Effect of phase angle of thickness variation on bending moments.

taken with the mean value $\bar{h}$ and w_i function, that need to be computed again, as they are affected by the sum on t.

Coupling between thickness profile and irregularity of the e.a.a., as defined by function w_i may be sought as well. Symmetric and anti-symmetric profiles may be studied. Effects of curvature of the e.a.a. is studied a part somewhere [2], but it is clearly a special case here.

Compression-flexure of beams upon contact to walls, in general, involves flexure in two planes, the horizontal and vertical, as both components of velocity are present in ice fields. The horizontal component of contact would add a horizontal H_0 component of internal force H, in the direction of the x-axis and a bending moment P, related to the in-plane curvatures. A pair of equations of equilibrium would then be added to Eqs. (1):

$$\begin{aligned} \partial_{,y}(H) &= -\psi\partial_{,y}(N) \\ \partial_{,y}(P) &= H - N\partial_{,y}(u) \end{aligned} \tag{43}$$

where $\psi = \partial_{,y}(u)$ represents the in-plane rotations, being u the x-components of displacement.

Considering the constitutive equation for P as being of the form, $P = -E'J\partial_{,yy}(u)$ where $J = \frac{\bar{h}t}{12}b_0^3$, and combining the above statements, it results that:

$$\partial_{,yy}[E'J\partial_{,yy}(u)] + N\partial_{,y}(\psi) = 0 \tag{44}$$

subjected to the additional boundary conditions,

$$\begin{array}{ll} y = 0; & H_0 = -\mu N_0 \\ & P_0 = 0 \end{array} \tag{45}$$

at origin, and,

$$\begin{array}{ll} y = L & u_L = 0 \\ & \partial_{,y}(u)_L = 0 \end{array} \tag{46}$$

which would entail a similar form of procedure to be applied to the horizontal problem. Again a full backward Euler procedure, in the form presented above, could be developed and applied simultaneously, or not. This conveys some additional dimension to the solution procedure developed and shows some advantages of this method with respect to some other largely used numerical methods, as the finite element method, of difficult application in semi-infinite problems, in particular containing variable thickness and initial curvature.

It should be pointed out that an elastic-damage model could be used as constitutive equation for the behavior of ice. In this case, load would be treated in incremental form, and a damage surface used to separate elastic, from damaged-elastic states. Increment corrections to the elastic modulus of the material, changed from E to E_D, on a sectional basis, would have to be implemented [7]. Though a lot more complicated, it could be made fit to the procedure developed here.

Acknowledgements: Contributions to the theme as well the insightful discussions on the part of prof. Tomasz Wiersbicki from M.I.T. are acknowledged.

References

[1] S. F. Ackely et al. *Thickness and Roughness Variation of Arctic Multi-year Sea Ice*. CREEL Report 78-13, New Hampshire, 1976.

[2] J. B. de Aguiar. *Bending Failure of Brittle Plates and Beams on an Elastic Foundation*. PhD thesis, M.I.T., Massachusetts, 1987.

[3] R. Frederking. Dynamic ice forces on an inclined structure. In *Physics and Mechanics of Ice, IUTAM Symposium*, pages 816–825, Copenhagen, Denmark, 1980.

[4] http://en.tek.norut.no/norut_teknologi/forskning/konstruksjonsteknikk/ice_mechanics.

[5] K. Kubicek and M. Morek. *Computational Methods in Bifurcation Theory and Dissipative Structures*. Springer-Verlag, New York, 1983.

[6] M. Mellor. Mechanical behavior of sea ice. Monography 83-1, Cold Regions Research and Engineering Laboratory, New Hampshire, 1983.

[7] A. Pralong, K. Hutter, and M. Funk. *Anisotropic damage Mechanics for Viscoelastic Ice*, volume 17 (5) of *Continuum Mechanics and Thermodynamics*. Springer-Verlag, 2006.

[8] M. Sayed and T. Carrieres. Overview of a new operational ice model. In *Proceedings of the 9^{th} Int. Offshore and Polar Eng. Conference*, pages 662–627, Brest, France, 1999.

[9] L. I. Slepian. On the modeling of ice cover fracture. In *Proceedings of the 1^{st} European Offshore Mechanics Symposium*, pages 499–504, Trondheim, Norway, 1990.

[10] V. N. Smirnov and A. I. Shushlebin. The results of studies of natural deformations of sea ice fields. In *Proceeding of the 1^{st} European Offshore Mechanics Symposium*, pages 512–516, Trondheim, Noway, 1990.

[11] B. D. Wright and G. W. Timco. A review of ice forces and failure modes on the Molikpaq. In *Proceedings of the 12^{th} IAHR International Symposium on Ice*, Trondheim, 1994.

[12] V. G. Zanegin, N. G. Khrapatyu, and T. Lyubinov. Investigation of sea ice shear properties. In *Proceedings of the 1^{st} European Offshore Mechanics Symposium*, Trondheim, 1990.